Effect of heat treatment on the dynamic impact response of Cu–Cr–Zr alloy manufactured by laser powder bed fusion

Nadia Azizi¹, Hamed Asgari², Mahyar Hasanabadi¹, Akindele Odeshi³, Ehsan Toyserkani^{1,*}

- ¹ Multi-Scale Additive Manufacturing Lab, University of Waterloo, Waterloo, ON, Canada
- ² Marine Additive Manufacturing Centre of Excellence, University of New Brunswick, Fredericton, NB, Canada
- ³ Department of Mechanical Engineering, University of Saskatchewan, Saskatoon, SK, Canada
- * hamed.asgari@unb.ca & asgari.ha@gmail.com

Abstract: This study investigates the effect of heat treatment on the dynamic impact behavior of a Cu–Cr–Zr alloy fabricated via high-power laser powder bed fusion (LPBF). Experiments utilized a split Hopkinson pressure bar (SHPB) setup with firing pressures of 100 kPa and 250 kPa, corresponding to maximum strain rates of 4400 s⁻¹ and 11300 s⁻¹ for as-built samples, and 1700 s⁻¹ and 4700 s⁻¹ for heat-treated samples. True stress-strain curves reveal a significant difference in strain accommodation mechanisms between as-built and heat-treated samples. Heat treatment markedly enhances the ultimate compressive strength (UCS) and work hardening rate under dynamic loading conditions, likely due to the Orowan strengthening mechanism by finely dispersed precipitates formed during heat treatment. The heat-treated samples exhibit continuous strength gains with increasing strain, reflecting pronounced strain hardening. In contrast, as-built samples show a plateau after reaching their UCS, where the activation of softening mechanisms, such as adiabatic shear band (ASB) formation, reduces the effectiveness of strain hardening. Despite the substantial changes in mechanical behavior, macro-texture analysis reveals minimal differences between as-built and heat-treated samples, suggesting that the performance disparities stem primarily from microstructural changes, such as precipitate formation and distribution in heat-treated samples, rather than shifts in crystallographic orientation.

Keywords: Additive manufacturing, Cu-Cr-Zr alloy, Dynamic impact behavior, Heat treatment, Laser powder bed fusion.

1. Introduction

Additive manufacturing (AM), particularly laser powder bed fusion (LPBF), has emerged as a promising technique for fabricating intricate Cu alloy components with high precision and complex internal features that are difficult to achieve with conventional methods. However, LPBF processing of copper alloys remains challenging due to the high reflectivity and thermal conductivity of Cu, often leading to defects such as porosity and incomplete melting [1]. Recent advances in LPBF technology, including higher laser powers and optimized scanning strategies, have enabled the successful production of Cu–Cr–Zr parts with improved properties [2].

The microstructure of LPBF-made Cu-Cr-Zr alloys is strongly influenced by rapid solidification, resulting in fine cellular substructures and significant supersaturation of Cr and Zr in the Cu matrix [3]. While this can enhance the strength of the alloy, the as-built microstructure is often not fully optimized for demanding service conditions. Post-processing heat treatments play a crucial role in improving the strength of these alloys by promoting the precipitation of fine Cr- and Zr-rich particles, which can hinder dislocation motion through the Orowan mechanism [4,5].

Despite these benefits, the influence of heat treatment on the dynamic mechanical behavior of LPBF-made Cu-Cr-Zr alloys remains insufficiently explored. Such knowledge is crucial for applications involving impacts or high-speed loading, where strain rate sensitivity and softening mechanisms like adiabatic shear band (ASB) formation become significant. While some studies have reported strain-rate effects in LPBF-made Cu alloys at moderate strain rates [6], data remain scarce for higher strain rates and for understanding how heat treatment alters dynamic deformation behavior.

Therefore, this study aims to investigate the effect of heat treatment on the dynamic impact response of a Cu-Cr-Zr alloy produced by high-power LPBF. Using a split Hopkinson pressure bar (SHPB) system, we examine both as-built and heat-treated samples at high strain rates, focusing on differences in strain hardening, softening mechanisms such as ASB formation, and the role of texture and microstructural changes on the dynamic mechanical characteristics of the samples.

2. Materials and methods

Plasma-atomized C18150 powder (Cu–1Cr–0.5Zr, wt.%) was processed on a customized AMCM EOS M290 LPBF machine equipped with a 1 kW Yb-fiber laser to produce cylinders (9.2 mm height \times 8 mm diameter) using our previously optimized parameters [7]. The particle size distribution of powder was $D_{10} = 16.8 \mu m$, $D_{50} = 37.6 \mu m$ and $D_{90} = 64.7 \mu m$.

Dynamic impact tests using a SHPB system were previously conducted on as-built Cu–Cr–Zr samples, with details reported in our earlier publication [8]. In this study, the same tests were performed on heat-treated samples to evaluate the effect of heat treatment on the alloy's dynamic response. For direct comparison, the as-built results from our previous work are included here alongside the results of heat-treated samples. All tests were carried out with the impact direction (ID) parallel to the building direction (BD) at firing pressures of 100 kPa and 250 kPa, with a minimum of four samples tested at each pressure to ensure repeatability, and average stress and strain values were reported for each condition.

Heat treatment was conducted at 450 °C for 3 h under vacuum (0.06 mbar) to facilitate the precipitation of fine Cr- and Zr-rich compounds, which contribute to strengthening the Cu–Cr–Zr alloy. This recipe was selected based on prior studies showing that aging treatments between 450 °C and 500 °C effectively promote the formation of nanoscale precipitates in LPBF-made Cu–Cr–Zr alloys, thereby enhancing both mechanical strength and electrical conductivity [9].

Microstructural analysis was carried out on cross sections perpendicular to the BD in undeformed samples and to the ID in deformed samples, using a TESCAN VEGA3 SEM equipped with a BRUKER electron backscatter diffraction (EBSD) detector. Macrotexture analysis of the samples was carried out using X-ray diffraction (XRD) with monochromatic Co- K_{α} radiation ($\lambda = 1.79$ Å), focusing on the (111), (200), and (220) planes.

3. Results and discussion

3.1. Dynamic mechanical response

Figure 1 compares the true stress–strain curves and work hardening rate curves for as-built (AB) and heat-treated (HT) Cu–Cr–Zr samples tested under dynamic loading. The AB results, taken from our previous study [8], were tested at strain rates of ~4400 s⁻¹ and ~11300 s⁻¹, corresponding to firing pressures of 100 kPa and 250 kPa, respectively. The HT samples, tested under the same firing pressures, reached lower strain rates of ~1700 s⁻¹ and ~4700 s⁻¹. This reduction happens because heat treatment can increase the strength and stiffness through precipitate formation, making the material less prone to deform under the same loading conditions.

As shown in Figure 1a, HT samples exhibit a significantly higher ultimate compressive strength (UCS) compared to AB samples at both strain rates. The HT samples continue to gain strength with increasing strain, reflecting pronounced strain hardening behavior, whereas the AB samples show a plateau after reaching their UCS, particularly at higher strain rates. This indicates the activation of softening mechanisms such as ASB formation in the AB condition.

Figure 1b confirms that HT samples sustain higher work hardening (WH) rates across a broader strain range. In both AB and HT conditions, there is a rapid drop in WH rate immediately after yielding. In AB samples, the WH rate continues to decrease steadily to near zero, leading to a stress plateau where strain hardening and softening mechanisms balance each other. In contrast, the HT samples show a slight increase in WH rate after the initial drop before it decreases again. This behavior is likely due to interactions between dislocations and finely dispersed precipitates formed during heat treatment [4,5], which contribute to sustained strain hardening.

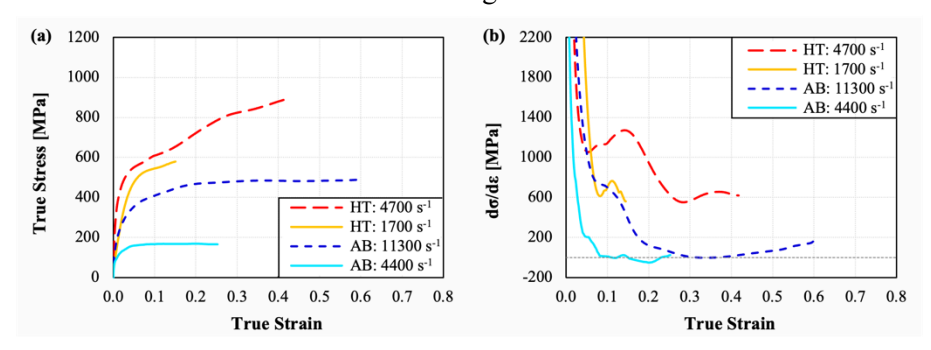


Figure 1. (a) True stress—true strain and (b) work hardening rate curves of as-built (AB) and heat-treated (HT) LPBF-made Cu–Cr–Zr alloy under different strain rates during SHPB test.

3.2. Microstructural observation

Figure 2 reveals the extent of deformation and the microstructural features of AB and HT Cu–Cr–Zr samples after dynamic impact. In the AB sample tested at ~11300 s⁻¹ (Figure 2a and 2b), significant macroscopic distortion and a dense network of intersecting ASBs are visible, indicating severe localized deformation and thermal softening. This behavior corresponds with the stress plateau seen in Figure 1a, reflecting limited strain hardening and early activation of softening mechanisms at high strain rates in the AB sample. The HT sample tested at ~4700 s⁻¹ (Figure 2c and 2d) shows less external distortion and fewer internal shear bands.

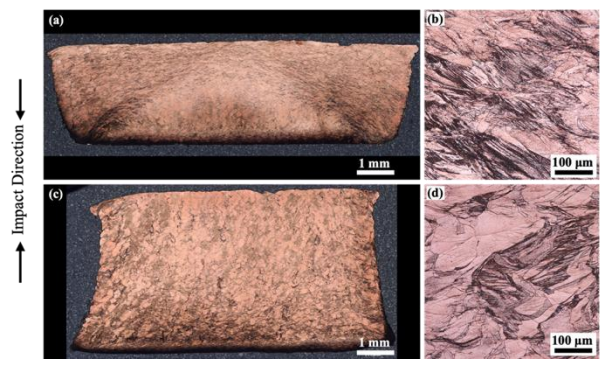


Figure 2. Optical microscopy (OM) images of LPBF-made Cu–Cr–Zr alloy after dynamic impact: (a,b) AB sample tested at \sim 11300 s⁻¹, and (c,d) HT sample tested at \sim 4700 s⁻¹.

Figure 3 shows EBSD maps for AB and HT samples. The grain size distributions in Figure 3a and 3d correspond to the undeformed state, revealing a slightly larger average grain size in the HT sample (172 µm) compared to the AB sample (144 µm). Despite this increase in grain size, the HT samples exhibit higher strength and improved strain hardening under dynamic loading (Figure 1). This behavior suggests that hardening from finely dispersed precipitates formed during heat treatment contributes more significantly to strengthening than grain boundary strengthening via the Hall–Petch effect. The precipitates effectively impede dislocation motion, enhancing strength even though grain coarsening might otherwise reduce it. The EBSD maps of the deformed AB samples (Figure 3b and 3c) display significant formation of deformation-induced features like ASBs, consistent with localized severe plastic deformation. In contrast, the EBSD maps of the deformed HT samples (Figure 3e and 3f) reveal fewer signs of intense localized deformation. This difference is partly due to the lower strain rates experienced by the HT samples under the same firing pressures. In addition, the HT condition likely contains finely dispersed precipitates that hinder dislocation motion and delay thermal softening, although the presence of these precipitates requires further confirmation by transmission electron microscopy (TEM) analysis.

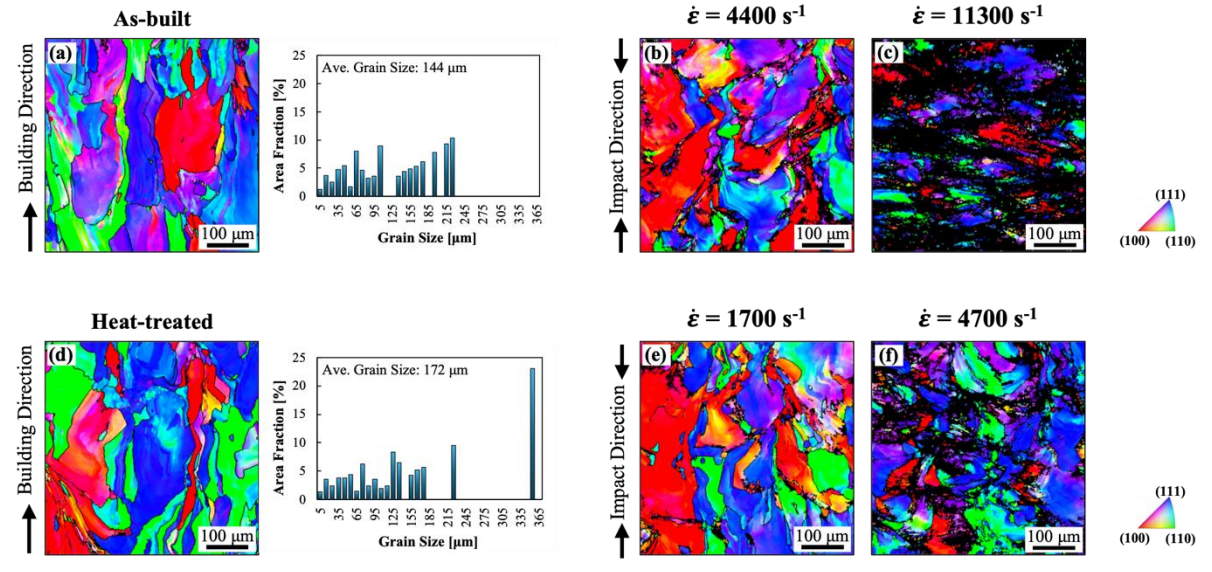


Figure 3. Inverse pole figure (IPF) maps of LPBF-made Cu-Cr-Zr alloy: (a-c) AB and (d-f) HT samples.

3.3. Macro-texture evolution

Figure 4 presents macro-texture pole figures for AB and HT samples in both undeformed and deformed conditions. In the undeformed AB condition (Figure 4a), strong textures are evident along the build direction (BD), reflecting the directional solidification typical of the LPBF process. The undeformed HT sample (Figure 4d) shows pole figures that appear very similar to those of the undeformed AB sample (Figure 4a). Although the HT condition exhibits slightly lower maximum intensities, the overall orientation patterns remain similar, indicating only minor texture weakening. Despite the slight grain coarsening introduced by heat treatment, no substantial differences are observed in the macro-texture. Even after dynamic deformation at strain rates of ~1700 s⁻¹ and ~4700 s⁻¹, the HT samples continue to show stable pole figure patterns, with maximum intensities nearly the same as in the undeformed HT samples. These observations suggest that the improved strength and strain hardening in the HT samples may be attributed primarily to precipitation strengthening rather than significant changes in crystallographic texture.

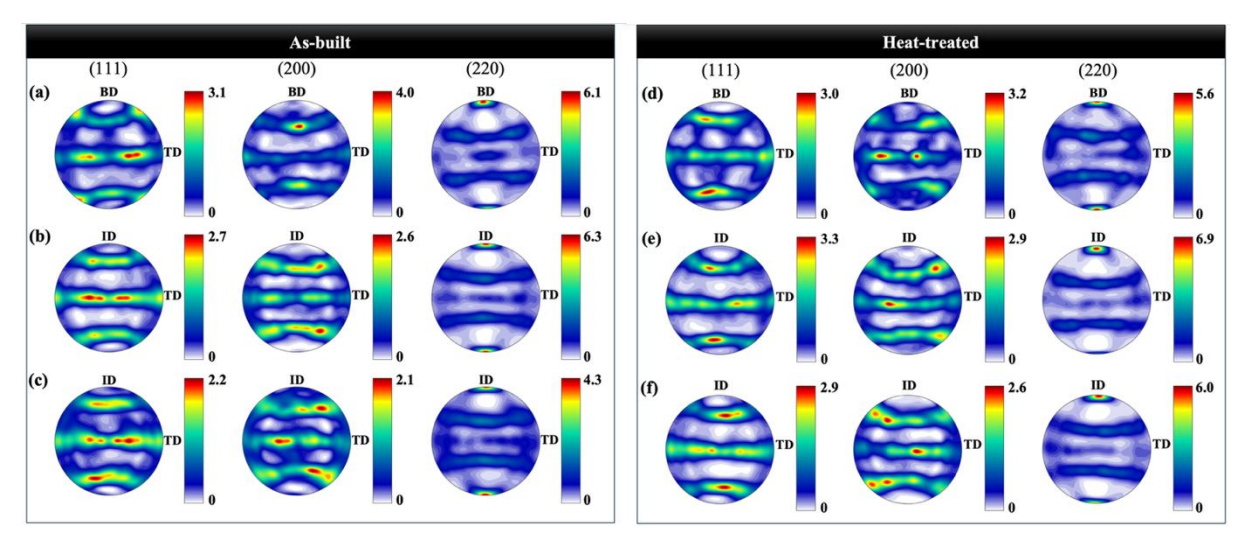


Figure 4. (111), (200), and (220) pole figures showing macro-texture of LPBF-made Cu–Cr–Zr alloy: (a–c) As-built samples: (a) undeformed and deformed at (b) \sim 4400 s⁻¹ and (c) \sim 11300 s⁻¹. (d–f) Heat-treated samples: (d) undeformed and deformed at (e) \sim 1700 s⁻¹ and (f) \sim 4700 s⁻¹. (BD = Building Direction; TD = Transverse Direction; ID = Impact Direction.)

4. Conclusion

This study investigated the effect of heat treatment on the dynamic impact response of Cu–Cr–Zr alloy fabricated by high-power LPBF. The following conclusions were drawn:

- Heat treatment improves the dynamic strength and strain hardening of LPBF-made Cu-Cr-Zr alloy while reducing softening effects such as ASB formation.
- HT samples show less severe localized damage under dynamic loading, indicating that precipitation strengthening from finely dispersed precipitates contributes significantly to the alloy's enhanced mechanical response.
- Macro-texture remains largely unchanged after heat treatment and dynamic loading, indicating that strength improvements arise mainly from microstructural changes rather than significant alterations in crystallographic orientation

5. Acknowledgments

We acknowledge the support of the Natural Sciences and Engineering Research Council of Canada (NSERC), funding reference number ALLRP 586345-24.

6. Conflicts of interest

The authors declare that they have no known competing financial interests or personal relationships that could have appeared to influence the work reported in this paper.

7. References

- [1] M. Roccetti Campagnoli, M. Galati, A. Saboori, On the processability of copper components via powder-based additive manufacturing processes: Potentials, challenges and feasible solutions, Journal of Manufacturing Processes, 72 (2021) 320–337.
- [2] T. X. Tang, X. Chen, F. Sun, L. Li, P. Liu, H. Zhou, S. Fu, A. Li, A study on the mechanical and electrical properties of high-strength CuCrZr alloy fabricated using laser powder bed fusion, Journal of Alloys and Compounds, 924 (2022) 166627.
- [3] T S. Zhang, H. Zhu, L. Zhang, W. Zhang, H. Yang, X. Zeng, Microstructure and properties in QCr0.8 alloy produced by selective laser melting with different heat treatment, Journal of Alloys and Compounds, 800 (2019) 286–293.
- [4] C. Wallis, B. Buchmayr, Effect of heat treatments on microstructure and properties of CuCrZr produced by laser-powder bed fusion, Materials Science and Engineering: A, 744 (2019) 215–223.
- [5] X. Tang, X. Chen, F. Sun, P. Liu, H. Zhou, S. Fu, The current state of CuCrZr and CuCrNb alloys manufactured by additive manufacturing: A review, Materials & Design, 224 (2022) 111419.
- [6] X. Qian, X. Peng, Y. Song, J. Huang, Y. Wei, P. Liu, X. Mao, J. Zhang, L. Wang, Dynamic constitutive relationship of CuCrZr alloy based on Johnson-Cook model, Nuclear Materials and Energy, 24 (2020) 100768.
- [7] N. Azizi, E. Jabari, M. Hasanabadi, E. Toyserkani, High-power laser powder bed fusion of Cu–Cr–Zr alloy: A comprehensive study on statistical process optimization, microstructure, and mechanical properties, Journal of Manufacturing Processes, 149 (2025) 931–954.
- [8] N. Azizi, H. Asgari, M. Hasanabadi, A. Odeshi, E. Toyserkani, On the microstructure and dynamic mechanical behavior of Cu–Cr–Zr alloy manufactured by high-power laser powder bed fusion, Materials & Design, 253 (2025) 113826.
- [9] C. Salvan, L. Briottet, T. Baffie, L. Guetaz, C. Flament, CuCrZr alloy produced by laser powder bed fusion: Microstructure, nanoscale strengthening mechanisms, electrical and mechanical properties, Materials Science and Engineering: A, 826 (2021) 141915.